THE ASTROPHYSICAL JOURNAL, 554:233–239, 2001 June 10
© 2001. The American Astronomical Society. All rights reserved. Printed in U.S.A.

A RAPID X-RAY FLARE IN THE RADIO-LOUD NARROW-LINE QUASAR PKS 0558−504

T. G. WANG,[1] M. MATSUOKA,[2] H. KUBO,[3] T. MIHARA,[4] AND H. NEGORO[4]

Received 2000 November 27; accepted 2001 February 9

ABSTRACT

We report the detection of a very short timescale flare in the radio-loud narrow-line quasar PKS 0558−504 that was observed using *ASCA*. The X-ray count rates increased and decreased by a factor of 2 in 33 minutes and possibly by 40% in as short a time period as 2 minutes during this flare, confirming with imaging detectors that such a flare event does occur in this object. The implied largest rate of change in luminosity in 0.8–10 keV alone, $dL/dt \simeq (1.8 \pm 0.4) \times 10^{42}$ ergs s^{-2}, is several times higher than the limit set for the isotropic emitting plasma around a Kerr black hole. Emission from either a relativistic boosting jet or a magnetic heated corona may explain such high radiative efficiency. A magnetic field with a strength of at least a few times 10^4 G is required in the latter case. The spectrum during this flare is significantly harder than an average spectrum. Three radio-loud narrow-line active galactic nuclei (AGNs) possess considerably smaller black holes than the radio-loud AGNs in bright-quasar survey, indicating that they are still in a rapid-growth phase of the black hole by accretion.

Subject headings: black hole physics — galaxies: active — galaxies: Seyfert — quasars: general — X-rays: galaxies

1. INTRODUCTION

Most active galactic nuclei (AGNs) show some flux variation. The timescale and amplitude depend strongly on the wavelength observed; particularly, the amplitude is larger and the timescale shorter in the X-ray band than in the optical band. Large amplitude variations over a timescale from minutes to hours have been reported for Seyfert galaxies and a particular beamed class of AGNs named blazars (e.g., Barr & Mushotzky 1986; McHardy 1989; Catanese & Sambrana 2000). A physical causality argument leads to either a very small emission region and/or relativistic beaming in these objects. In fact, combined with the large energy output in the X-ray band, this is considered strong evidence for their extremely high radiative efficiency, which leads to the general picture of massive black hole accretion for AGNs (e.g., Fabian 1979; Rees 1984).

Among various types of AGNs, only Seyfert galaxies and BL Lac objects are well studied for short-timescale X-ray variability. This is partly due to their brightness in the X-ray band. Nandra et al. (1997) presented a systematic analysis of the variability of X-ray flux for a sample of broad-line Seyfert galaxies observed by *ASCA* and found that the X-ray variability amplitude is well anticorrelated with the luminosity. Leighly (1999a) demonstrated that a subclass of Seyfert galaxies, called narrow-line Seyfert 1 galaxies (NLS1s;[5] Osterbrock & Pogge 1985; Goodrich 1989), also follows an anticorrelation of amplitudes with luminosities, but, for a given X-ray luminosity, NLS1s show much larger variability amplitudes. This finding confirms the suspicion, based on the studies of individual objects, that NLS1s are more variable than normal Seyfert galaxies. Examples of large variations can be found in the literature (e.g., Boller, Brandt, & Fink 1996; Forster & Halpern 1996; Otani, Kii, & Miya 1996).

PKS 0558−504 ($z = 0.137$, $m_B = 14.97$) is one of the rare radio-loud NLS1-type objects. Remillard et al. (1992), using the *Ginga* satellite for observation, reported the detection of a rapid flare in which the X-ray flux increased by 67% in 3 minutes, and they suggested that the X-ray emission is enhanced by relativistic beaming. However, *Ginga*'s lack of imaging capacity makes this result somewhat questionable, as the flare might be due to a neighboring source. Recently, Gliozzi et al. (2000) observed this object with the *ROSAT* HRI in the soft X-ray band and also found strong persistent variations in the soft X-ray band. But their $\Delta L/\Delta t$ is considerably smaller than that reported by Remillard et al. (1992). In this paper, we report the detection of a rapid energetic flare in this object with imaging detectors.

2. OBSERVATION AND DATA REDUCTION

PKS 0558−504 was observed with *ASCA* (Tanaka, Inou, & Holt 1994) on 2000 January 31 with an effective exposure time of 37.4 ks. The Solid-State Imaging Spectrometer (SIS) was operated by mixing faint and bright 1 CCD mode, and the Gas Imaging Spectrometer (GIS) was operated on pulse-height mode. For the SIS, the faint-mode data were converted into bright data and then combined with the bright-mode data. The data reduction was performed in the standard way by using FTOOLs v4.2. Hot and flickering pixels were removed from the SIS data. To check the reliability of the scientific results, we have chosen both strict data-screening criteria and standard ones (see The *ASCA* Data Reduction Guide, version 2). Both criteria yield consistent results, particularly for the flare profile. Since the standard criteria yield slightly better statistics in the X-ray spectrum, we will present these below. After standard screening, the net exposure times are 37.4 ks and 25.9 ks for the GIS and SIS detectors, respectively.

The source counts were extracted from a circular region of 3′.5 and 5′.0 radius for SIS and GIS, respectively. The background counts were estimated from the off-source region at the same off-axis angle and area for each of the

[1] Center for Astrophysics, University of Science and Technology of China, Hefei, Anhui 230026, China; twang@ustc.edu.cn.
[2] Space Utilization Research Program, NASDA, 2-1-1 Sengen, Tsukuba City, Ibaraki 305-8505, Japan.
[3] Department of Physics, Faculty of Science, Kyoto University, Sakyo-ku, Kyoto 606-8502, Japan.
[4] The Institute of Physical and Chemical Research (RIKEN), 2-1 Hirosawa, Wako, Saitama 351-0198, Japan.
[5] We do not distinguish between NLS1 and narrow-line quasars; we call them simply NLS1.

GIS detectors and from the source-subtracted region of the same chip of CCD for each of the SIS detectors. The background accounts for about 5% of the total counts for both SIS and GIS. The average net source count rates, after correcting for background, are 0.470 ± 0.003, 0.598 ± 0.004, 1.009 ± 0.007, and 0.820 ± 0.005 counts s^{-1} for GIS2, GIS3, SIS0, and SIS1, respectively.

Light curves were extracted for the source and background for each detector. For both GIS detectors, the background count rate is nearly constant during the observation; therefore, an average count rate is used to estimate the background level. For the SIS detectors, the extracted background rate seems to be correlated with the source owing to contamination of the AGNs. Therefore, it is only an upper limit to the true background and is used only for spectral analysis. Since smaller extraction radii in the real sky are used for SIS detectors, the fraction of background light is estimated to be smaller than in the GIS case. We will ignore the background contribution to the SIS count rate during the light-curve analysis.

The X-ray spectra were rebinned to at least 25 counts bin^{-1}. For the SIS spectrum, the response matrices appropriate for the date of the observation (thus accounting for the decline of the energy resolution as a function of time) were made using the script *sisrmg*. For the GIS spectrum, the 1994 response matrices (gis2v4_0.rmf and gis3v4_0.rmf) were adopted. Ancillary response files were made for each detector using *ascaarf*. The *ASCA* data preparation and the spectral analysis were performed using version 1.4 of the XSELECT package and version 10.01 of XSPEC.

3. SPECTRAL AND TEMPORAL ANALYSIS

3.1. *The Spectral Properties*

Since the efficiency of SIS detectors has decreased owing to radiation damage and the current calibration files do not account for this, we only used SIS spectra above 0.8 keV. The GIS spectra below 0.8 keV are not well calibrated and will not be used in the spectral fit. The X-ray spectra in the full *ASCA* band cannot be adequately described by an absorbed power law with $\chi^2/\mathrm{dof} = 1058/924$, which is accepted at a probability of only 1×10^{-3}. There are systematic deviations at low energies. In addition, the fitted column density $[(2.4 \pm 1.2) \times 10^{20}\ \mathrm{cm}^{-2}]$[6] is significantly lower than the Galactic value ($4.5 \times 10^{20}\ \mathrm{cm}^{-2}$).

In order to see if this is a result of the soft X-ray excess that was noticed in the *Ginga* spectrum (Remillard et al. 1992), we initially fitted the spectrum above 2.0 keV. A single power law with Galactic absorption provides a good fit to the joint GIS and SIS spectra ($\chi^2/\mathrm{dof} = 631/636$). The best-fitted photon index ($\Gamma = 2.20^{+0.02}_{-0.04}$) is slightly flatter than the previous fit ($\Gamma = 2.25^{+0.02}_{-0.03}$). This spectral index matches well the one obtained by Leighly (1999b) for a 1997 observation, suggesting no significant variation in the spectral index between the two observations. Extrapolating this fit to low energies shows excesses in the soft X-ray band (Fig. 1), particularly below 1.2 keV. The excess is larger in the GIS spectra than in the SIS spectra and is also larger in the SIS0 than in the SIS1, possibly indicating the decreasing efficiency of SIS already evident in the energies just below 1.2 keV. If the soft excesses are modeled with blackbody emission, the best fit yields $kT = 0.22 \pm 0.02$ keV and a normalization of $3.4^{+1.3}_{-1.0} \times 10^{-5}$. The latter corresponds to a flux in 0.8–2 keV of 2.1×10^{-12} ergs sec^{-1} cm^{-2}. Although this fit is better than the single–power-law fit by $\Delta\chi^2 = 31$, it is still statistically acceptable only at 1% probability ($\chi^2/\mathrm{dof} = 1027/923$). After carefully examining the residuals, we find that the counts of the SIS detector are significantly lower than those of the GIS at energies below 1.15 keV. This is most likely caused by the degeneration of the SIS sensitivity at low energies. In fact, the fit is acceptable (926/894, $P_r = 0.22$) when the SIS data below 1.2 keV are ignored. This fit yields $kT = 0.13^{+0.03}_{-0.02}$ keV and a normalization of $1.50^{+1.10}_{-0.53} \times 10^{-4}$. The photon index for this fit is $2.22^{+0.02}_{-0.03}$, which is similar to that derived for fitting the 2–10 keV spectrum.

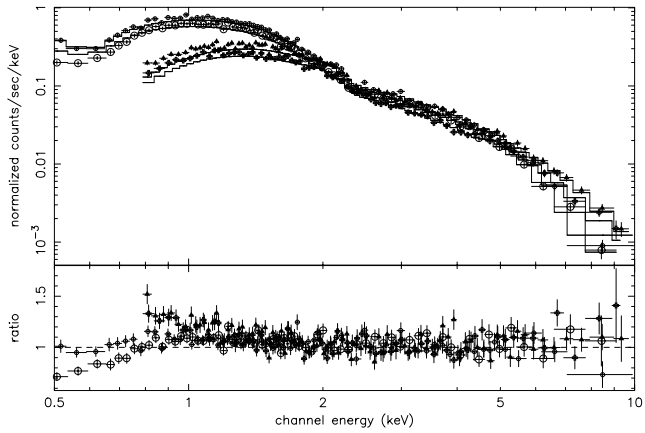


FIG. 1.—*ASCA* spectra of PKS 0558−504 (*upper panel*) and the ratios of data to a best power-law fit to the 2–10 keV band data (*lower panel*). SIS0, SIS1, GIS2, and GIS3 data are marked with small circles, large circles, crosses, and triangles, respectively. Systematic excesses over the power-law are clearly present. The SIS spectrum is plotted to 0.5 keV for the purpose of illustrating the degeneration of the SIS efficiency.

Recently, O'Brien et al. (2000) found that the soft excess extends up to 3 keV from their much higher quality *XMM* spectrum and can be modeled as multiple-temperature blackbody emission. The spectral slope of the power-law component is 0.9, fully consistent with those found for other Seyfert 1 galaxies. The steep hard X-ray component found in the *ASCA* spectrum could be a result of the contamination of the spectroscopically unresolved soft X-ray excess in the *ASCA* 2–10 keV band.

No iron K line is detectable with the *ASCA* data. An upper limit of equivalent width for a narrow Gaussian line at 5.5 or 5.7 keV (6.4 and 6.7 keV in the source rest frame) is 40 eV, consistent with *XMM* results (O'Brien et al. 2000).

3.2. *Temporal Properties*

Figure 2*a* shows the combined GIS and SIS light curves for the count rates in 0.8–10 keV and 0.6–10 keV bands, respectively. A large energetic flare started shortly after the observation. The count rate increased from 0.54 ± 0.02 counts s^{-1} to 1.10 ± 0.04 counts s^{-1} in about 2000 s, and then it decreased to 0.50 ± 0.02 counts s^{-1} in about 3500 s. Since there is an observation gap between these two measurements, the real variations might be even faster.

We have examined possible contamination sources. The background count rates are stable and are at a level of only a few percent of the source count rates during the observation. Concerning the impact of particle background, we

[6] Uncertainties are given at 90% confidence level for one interesting parameter for all the spectral parameters given in this section.

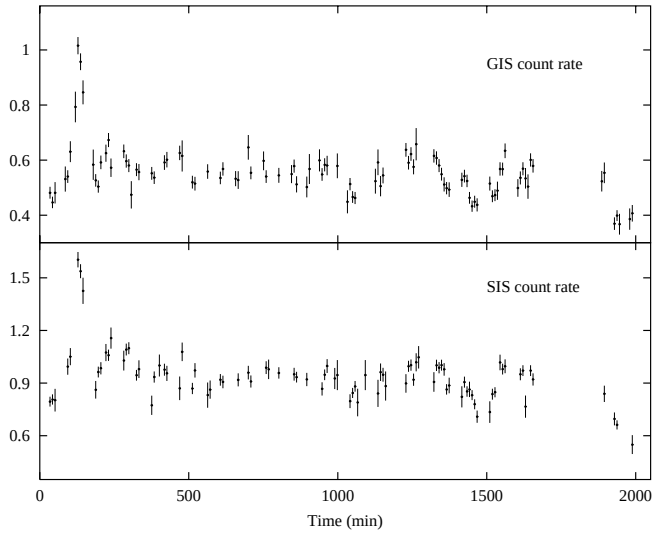


FIG. 2 *a*

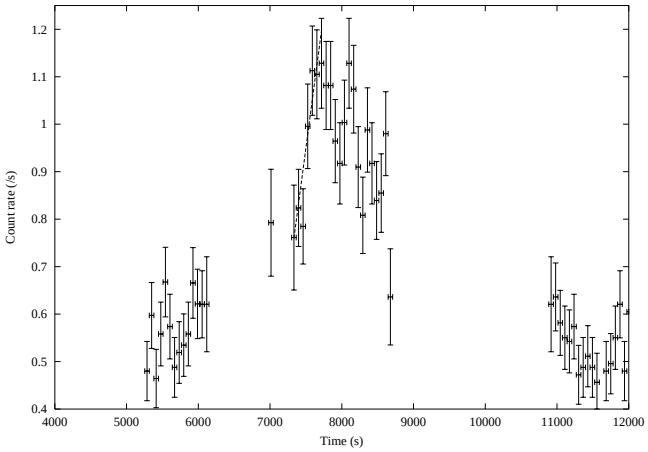


FIG. 2 *b*

FIG. 2.—(*a*) *ASCA*, SIS, and GIS light curves for PKS 0558−504. The count rate is binned in 256 s bins, and the data from two SIS and two GIS detectors have been combined. The background count rate, which is about 5% of the total, has not been subtracted. (*b*) Flare is clearly present in the both SIS and GIS data and is shown in enlarged scale for GIS data. A dashed line represents the linear fit of the steep rising part the light curve for estimation of the rate of change in the count rate.

applied strict screening criteria to the GIS data (refer to The *ASCA* Data Reduction Guide, version 2) and the flare structure remained. The source position measured in the *ASCA* GIS image is $05^h59^m41\overset{s}{.}1$, $-50°27'24\overset{''}{.}1$ (equinox 2000), which has an offset of $\Delta\alpha = 1\overset{'}{.}58$ and $\Delta\delta = 0\overset{'}{.}39$ from the NASA/IPAC Extragalactic Database (NED) position of PKS 0558−504. However, after correcting for a temperature-dependent deviation of the attitude solution (Gotthelf et al. 2000), the *ASCA* position deviates from the NED one by about 13″, which is within the 90% error circle (24″) of the GIS. We also noted that the image extracted for the events collected during the flare phase has a position of $09^h59^m40\overset{s}{.}4$, $-50°27'16\overset{''}{.}8$, which is only 11″ away from the position of the source in the total observation for the GIS. This analysis concludes that any confusing source should be within 20″ of the PKS 0558−504. The analysis of the SIS data gives a similar conclusion, but we do not give detailed numbers here because our main analysis below concentrates on the GIS curve.

The SIS curve is similar to the GIS one. The flare is also clearly present in the SIS data. Owing to different screening criteria applied to the SIS and GIS, the SIS data just before the peak of the flare are not available. Thus, the flare profile is less well defined than in the GIS curve.

The flare is shown with increased time resolution (GIS 64 s bins) in Figure 2*b*. Clearly, the source shows variability on short timescales of 10^2 s. A χ^2 test on the constancy of count rate for the second group of data in Figure 2*b* gives a $\chi^2/\mathrm{dof} = 45.6/21$, which is at a probability $P_r = 0.002$ by chance. The preflare has a mean count rate of 0.53 ± 0.02 counts s^{-1} for an interval of 650 s. Unfortunately, there is a 1000 s gap just before the onset of the flare. Nevertheless, the flare rose very fast. The count rate increased from 0.82 ± 0.05 counts s^{-1} (average over 3 bins) to the peak count rate 1.14 ± 0.05 counts s^{-1} (average over 3 bins) in less than 128 s. The statistical significance of this change is about 4.5 σ. This gives a rate of change in the count rate ΔCR counts s^{-2}. A more subjective estimate of the rate by linear fit to the rising part of the curve (first seven points in the second group of data, see Fig. 2*b*). This gives a rate of $\Delta\mathrm{CR} = (1.14 \pm 0.28) \times 10^{-3}$ counts s^{-2}, a factor of 2 lower than the one from direct visual inspection. We will quote the latter, more conservative number in later discussion. The source was then dimming with possible flicker until the end of this orbit. The presence of the second peak is probably also real since it appears in the SIS curve as well. The flux returns to the preflare level at the beginning of the next orbit observation.

We define two bands based on the spectral range of the soft X-ray excess (see § 3.1). The energy ranges are 0.8–2.0 keV and 2.0–10 keV for soft and hard bands for GIS data, respectively. The soft band extends to 0.5 keV for the SIS data since there is a substantial fraction of counts in the energy range 0.5–0.8 keV. The light curves for these two bands were extracted in order to examine possible spectral variations during the flare. The flare is seen in both bands. However, it shows a larger amplitude and decays faster in the hard band than in the soft band. The ratios of the count rate for the flare peak to the preflare for the soft and hard bands are 1.70 ± 0.13 and 2.13 ± 0.17, respectively. There is no significant decrease in the count rate of the soft band during the flare orbit ($\chi^2/\mathrm{dof} = 3.4/3$ and $P_r > 0.3$ for a constant count rate in the last 1024 s during the flare orbit) in contrast to the clear rising and fading in the curves of the hard band ($\chi^2/\mathrm{dof} = 15.0/3$ and $P_r \simeq 0.002$ for the same χ^2 test; see Fig. 3).

We examine whether there is a correlation between the hardness ratio and the total count rate and whether the flare follows the same correlation. The hardness ratio is the ratio of count rates in the 2–10 keV band and 0.8–2.0 keV band. In order to achieve a reasonable signal-to-noise ratio for each bin, we use 1024 s binning light curves. The hardness ratio is weakly anticorrelated with the total count rate for normal variations. A Spearman rank correlation analysis gives a correlation coefficient of $r = -0.371$ ($n = 62$), for which the probability for null hypothesis is $P_r = 0.3\%$ for the GIS data (we have ignored these data points with uncertainty in the ratios larger than 0.15). In

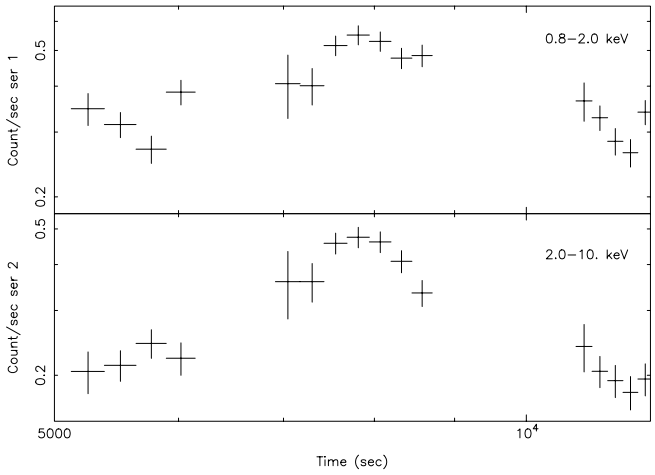


FIG. 3.—Hard and soft X-ray GIS light curves for the time period from preflare to postflare. Notice that the soft band shows a different flare profile than the hard one. The SIS curves show a similar character (not shown here).

Figure 4, we add the hardness ratios for the flare phase, which is binned with 512 s binning. The flare is distinguished from others for having a large hardness ratio and a large count rate (Fig. 4). In fact, the hardness ratio of the first three data points of the flare phase are among the largest, and the last data point of the flare returns to the average hardness ratio. If the spectrum during the flare is a power law, the power-law indices are about 1.9 for the first three points of the flare and 2.2 for the last point of the flare (Fig. 4). It is not clear whether the decreasing hardness ratio indicates a time delay between the two bands. Cross-correlation analysis does not find any definite delays between the soft X-rays and the hard X-rays.

Since the first three data points during the flare imply a spectral index of 1.9 (see Fig. 4), which is significantly harder than the mean spectral index in the 2–10 keV band, the change in the hardness ratio cannot be explained by the change in relative contribution of the soft excess alone. The

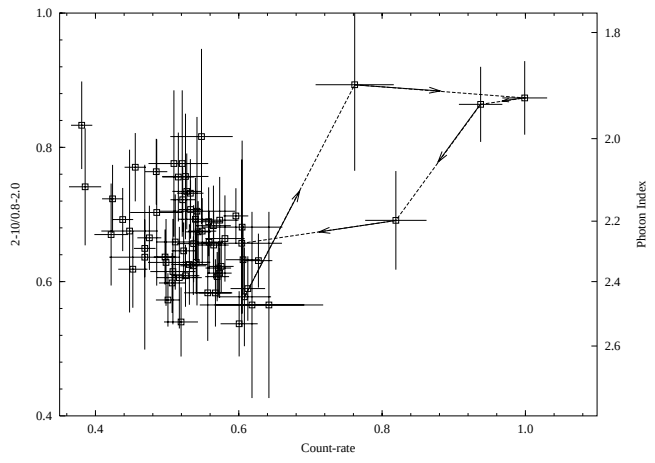


FIG. 4.—Plot of hardness ratio against the total count rate in the 0.8–10 keV band for the SIS data. The right y-axis also shows the corresponding photon index, assuming a power-law spectrum. The data points during the flare and surrounding it are connected with a line, and the arrows indicate the proceeding direction of the flare. Notice that the flare shows a clockwise-loop structure on the plot.

spectrum in the 2–10 keV band must also have changed. However, if the hard X-ray spectrum is as flat as $\Gamma = 1.9$, as suggested by *XMM* observations (O'Brien et al. 2000), then during the large flare the X-ray emission is dominated by the hard power law.

4. DISCUSSION

We observed a rapid flare in the PKS 0558−504 during which the X-ray count rate increased by a factor of nearly 2 in 33 minutes and possibly by 40% in as short as 2 minutes. This result independently confirms the existence of a rapid flare in this object obtained by *Ginga* (Remillard et al. 1992) and further suggests that the flare is repetitive. *ROSAT* HRI observations also found that the object is highly variable in the soft X-ray band, but no clear rapid-flare event was seen (Gliozzi et al. 2000). This might be a result of the relatively flat spectrum during the flare phase (a much lower amplitude in the soft X-ray band), and/or the low photon-collecting area of the *ROSAT* HRI, or, it does not happen to catch a flare. Neither the *ASCA* observation in 1999 nor the *XMM* observation in 2000 (Gliozzi et al. 2001) detected a rapid flare. The total exposure time, calculated by summing the exposure times of *Ginga*, *ASCA*, and *XMM* observations, is about 150 ks, in which rapid flares were detected twice. This suggests that rapid flares occur relatively frequently in this object.

The fastest variation during the rise-of-flare phase suggests a rate of change in the count rate of $\Delta\mathrm{CR} = (1.14 \pm 0.28)10^{-3}$ counts s^{-2} in a linear fit. Assuming that the X-ray spectrum can be described by a power law, the flare has a spectrum with a photon index of $\simeq 1.9$ from its hardness ratio; the rate of change in the count rate yields a $\Delta L/\Delta t = (1.8 \pm 0.4) \times 10^{42}$ ergs s^{-2} in the 0.8–10 keV band (assuming $H_0 = 75$ and $q_0 = 0.5$) if the X-ray emits isotropically. Note that this value is similar to the one obtained during the *Ginga* observation. Since the flare spectrum must not be limited in the 0.8–10 keV band, the actual $\Delta L/\Delta t$ should be larger. If the hard X-ray spectrum extends to energy levels as high as 100 keV then the flare luminosity will be a factor of 2 higher. Notice that there is a limit on $\Delta L/\Delta t \leq 2 \times 10^{42}\eta$ ergs s^{-2}, where η is the efficiency of converting matter to radiation, for spherically distributed plasma, whose opacity is dominated by Thomson scattering (e.g., Guilbert, Fabian, & Rees 1993). The $\Delta L/\Delta t$ given above yields an efficiency of $\eta = 0.9 \pm 0.2$, which exceeds the limit for accretion even onto a Kerr hole. This was interpreted as evidence supporting the relativistic beaming in this object by Remillard et al. (1991).

4.1. *A Flare from Relativistic Jets?*

Since PKS 0558−504 is a radio-loud quasar, we will first examine the possibility that the flare is produced in relativistic radio jets. There is evidence that the X-ray is dominated by the emission from relativistic jets in radio-loud quasars (e.g., Worral & Wilkes 1990). Relativistic beaming is expected naturally in this case if the jet beams toward us. We noticed that the broadband optical-UV to X-ray spectrum is flat with a spectral index $\alpha = (1.1\text{–}1.3)$, in the range for radio-loud quasars (Brinkmann, Yuan, & Siebert 1997). Lack of a detectable Fe Kα line is also consistent with the X-ray observations of other radio-loud quasars. However, the X-ray spectrum of PKS 0558−504 in the 2–10 keV band is much steeper than that of a typical radio-loud quasar. It resembles those of high-energy peaked BL Lac

(HBL) objects, in which the X-ray spectrum is believed to be the tail of the synchrotron emission of the relativistic jets (e.g., Kubo et al. 1998). Furthermore, we notice that HBL objects also show a loop structure on the plane-of-hardness ratio versus the count rate during flares, possibly owing to the synchrotron cooling of electrons (e.g., Kataoka et al. 2000). Since the jet in a BL Lac object is thought to beam toward the observer, this meets the requirement of relativistic boosting. Even for BL Lac objects, such fast (faster than 10^3 s) flares were only reported in a few cases (Feigelson et al. 1986; Catanese & Sambrana 2000).

However, PKS 0558−504 is not a BL Lac object. It has prominent emission lines rather than the weak or nondetectable emission lines typical of a BL Lac object. In addition, PKS 0558−504 shows a steep radio spectrum with a 2.7–5 GHz spectral index of 0.88 (Wright & Otrupcek 1990; Gregory et al. 1994; Wright et al. 1994), contrary to the flat radio spectra of BL Lac objects; and, finally, the fact that the continuum of PKS 0558−504 is dominated by a big blue bump extending into the soft X-ray band suggests that it is unlikely that the nonthermal emission from jets overwhelms the nucleus emission by a large factor even in the X-ray band (O'Brien et al. 2000).

This does not rule out the possibility that the X-ray flare is induced by a relativistic jet while the emission is from the nucleus in the normal state. The fact that the X-ray spectrum during the flare phase tends to be flatter than in the average spectrum is consistent with its being from a distinct component. If the nucleus component has a flux similar to the average value, half of the count rate during the flare must come from the nucleus component, since the count rate during the flare is greater than during the normal state by a factor of 2. If this is the case, the flare component could be as flat as a power law with an index of 1.6.

4.2. *A Magnetic Flare?*

Given that there is no evidence associating the flare with radio jets in PKS 0558−504, we consider the possibility that it arises from the nucleus. Rapid variations in the X-ray band are common even in radio-quiet NLS1s, where no relativistic radio jets have been observed. Some extreme variations in objects such as PHL 1092 and IRAS 13224−3809 also suggest a radiative efficiency larger than those setting by the accretion of matter onto Schwarzschild black holes (e.g., Forster & Halpern 1996; Boller et al. 1996). As discussed by Guilbert et al. (1983), either nonspherical geometry or continuous acceleration of electrons can generate a large effective radiative efficiency. Particularly interesting is a magnetic coronal model, in which particles in the corona are continuously heated by magnetic reconnection, up-scattering the soft photons from the accretion disk into X-rays. Since the magnetic field does not contribute to the scattering opacity, this would raise the effective efficiency. If the energy is prestored in the magnetic field co-region with the emission plasma, the effective efficiency can be as large as $\eta \leq B^2/(8\pi\rho_0 c^2)$, where B is the strength of the magnetic field and ρ_0 is the mass density of the corona region. When the magnetic energy density approaches that of the rest mass, the η is order of 1. In this model, the X-ray spectral index is a function of the particle temperature and the optical depth of the corona. The temperature is determined by the balance of the heating and cooling rate, since Compton cooling is very effective for hot electrons in NLS1s as estimated below.

The electron energy-loss rate is

$$\frac{dE}{dt} = n_e \int \frac{U_\nu}{h\nu}\, c\sigma_{\rm T}\, \frac{4kT - h\nu}{m_e c^2}\, h\nu d\nu\ , \tag{1}$$

where U_ν is the specific radiation energy density at frequency ν, $\sigma_{\rm T}$ the Thomson cross section, m_e the rest mass of an electron, and T the electron temperature. If the average photon energy is much smaller than the thermal energy of hot electrons, then we can ignore the process of transferring photon energy to an electron. One can easily get a cooling timescale for hot electrons using the following formula:

$$\tau_c \simeq \frac{3\pi}{2}\, \frac{m_e c^2}{\sigma_{\rm T}}\, \frac{r^2}{L} = 58 L_{45}^{-1} r_{14}^2 \text{ s}\ , \tag{2}$$

where L is the luminosity in the UV and soft X-ray bands, r the size of the continuum emission region, $L_{45} = L/(10^{45}$ ergs s$^{-1})$, and $r_{14} = r/(10^{14}$ cm).

For typical emission-region luminosity and size, this timescale is rather short compared to the typical flux-variation timescale. Therefore, if hard X-ray emission is produced by the Compton scattering process, the fading time (order of 10^3 s) seems irrelevant to the electron cooling process and is more likely a result of variations in electron heating rates, e.g., magnetic reconnection rate or even the coupling time of electrons with ions.

If a flare is energized by magnetic reconnection, the total energy stored in the magnetic field $(B^2/8\pi)l^3$ must not be less than the total energy emitted during the flare $(\Delta L \Delta t)$, where l is the scale of the magnetic field and ΔL and Δt are the luminosity and the duration of the flare. When an anomalous resistivity is introduced, the magnetic reconnection takes place and it spreads at the speed of Alfvén velocity, $v_{\rm A} = (B^2/4\pi\rho)^{1/2}$. The global magnetic field dissipation time should be not shorter than $l/v_{\rm A}$. Notice that converting a significant power into X-rays needs a Thomson optical depth $\tau_{\rm T}$ on the order of 1. Putting all of these parameters together, one yields the timescale of variability

$$\Delta t \geq 4 \times 10^3 \Delta L_{45}^{1/5} B_4^{-8/5} \tau_{\rm T}^{3/5} \text{ s}\ , \tag{3}$$

where $B_4 = B/(10^4$ G), $\Delta L_{45} = \Delta L/(10^{45}$ ergs s$^{-1})$; Δt is sensitive to magnetic field strength, but only weakly depends on luminosity. For the fastest variation during the rising phase of the flare, $\Delta L = 5 \times 10^{44}$ ergs s^{-1} in $\Delta t = 280$ s (using the linear-fit result), one yields $B \geq 5 \times 10^4 \tau_T^{3/8}$ G for the flare region. If part of the energy dissipated via magnetic reconnection is converted into kinetic energy, bulk motion of the flaring material results (Beloborodov 1999). The bulk motion would boost the apparent variability if it was toward the observer. However, the flare material is only mildly relativistic as estimated by Beloborodov (1999), and this would not seriously affect the magnetic field given above.

The strength of the magnetic field in an accretion disk is in principle limited by equipartition with the disk pressure. A stronger magnetic field would rise buoyantly from the accretion disk, leading to a magnetically confined corona (Galeev, Rosner, & Vaiana 1979). Mineshige et al. (2000) argued that the magnetic field is large in the NLS1s owing to large amounts of pressure caused by trapped photons in the inner region (radiation-pressure dominated) of a slim disk. By requiring $P_{\rm mag} \leq P_{\rm disk} \simeq P_{\rm rad} = aT^3/3$, one can estimate the disk temperature of the region that produced the flare. This gives a $kT_{\rm disk} \geq 38$ eV, which is somewhat

lower than that of the lowest temperature component in the O'Brien et al. (2000) multiple-blackbody model derived from the broadband *XMM* spectrum. This perhaps explains why a rapid energetic flare could only be observed in NLS1s with extremely steep soft X-rays.

4.3. *Black Hole Masses in Radio-Loud NLS1s*

There is growing evidence for the existence of larger black holes (BHs) in radio-loud quasars than in radio-quiet ones. By assuming that the line-emitting gas is virialized, Laor (2000) derived BH masses of the radio-loud quasi-stellar objects (QSOs) above $10^9\ M_\odot$, which are significantly larger than those in radio-quiet QSOs. This result is in line with the recently identified correlation between the mass of the central BH and that of the bulge (Magorrian et al. 1998; Gebhardt et al. 2000; Ferrarese & Merritt 2000), together with the fact that the radio-loud objects are hosted by elliptical galaxies. It is not yet understood how jet formation is related to the mass of the central BH in AGNs; galactic BH binaries also show superluminal radio jets, but their typical mass is around $10\ M_\odot$.[7] McLure et al. (1999) found that both luminous radio-loud and radio-quiet quasars reside in elliptical galaxies, suggesting the existence of massive BHs in both types of QSO.

On the other hand, it was suggested that the formation of jets might be related to low accretion rates such as in advection-dominated accretion flow (e.g., Rees et al. 1982; Blandford & Begelman 1999) and/or to the spin of the BH (Blandford & Znajek 1977). It is worthy to mention that the radio emission from BH X-ray binaries appears to be strong in the low state (Fender 2001), while it is suppressed in the high state.

However, evidence shows that the PKS 0558−504 possesses a low-mass BH and has a high accretion rate. The Hβ width of this object is around 1250 km s^{-1} (Corbin 1997), and the optical continuum luminosity is $\nu L_\nu(5100\ \text{Å}) \simeq 2.2 \times 10^{45}$ ergs s^{-1} from the V magnitude, corrected for Galactic reddening (Corbin & Smith 2000). By adopting the empirical broad-line region (BLR) size versus optical luminosity relation, $R_{\rm BLR} \simeq 18.65[\lambda L_\lambda(5100\ \text{Å})/10^{44}\ \text{ergs s}^{-1}]^{0.7}$ (Kaspi et al. 2000), and, further assuming that the BLR is virialized, we can derive a central BH mass of $4.5 \times 10^7\ M_\odot$. With this BH mass, the object is emitting at super-Eddington luminosity. Note that the mass of the central BH is far less than the masses seen in the radio-loud quasars in the PG sample (Laor 2000), which were inferred with the same method. We wish to point out that the V magnitude of PKS 0558−504 is 14.97, and its $B-V$ and $U-B$ values are similar to those of 3C 273. If it were in the north sky, it would be selected as a PG QSO as well.

There are a number of uncertainties in the above estimation of the mass. We have used the empirical $R_{\rm BLR}$-$L_{\rm opt}$ relation. The BLR is photoionized by far-/extreme-UV photons, and the size may scale more adequately with the ionizing continuum than with the optical luminosity. Since PKS 0558−504 shows a very big blue bump as detected by *XMM* in optical-UV and broadband X-rays (O'Brien et al. 2000), it has more ionizing flux than a typical QSO with similar optical luminosity, and thus a larger BLR. To give the order of magnitude of this correction, we estimate an optical-UV spectral slope $\alpha \simeq 0.1$, which is 0.4 lower than typical QSO value. If this spectrum extends to the Lyman limit, there is a factor of 2 more flux at this λ912 than at typical QSO spectra. This will only increase the mass of the BH by a factor of 1.5, which is still far less than the masses of BHs in radio-loud PG QSOs. Since the increase in ionizing photon flux also raises the bolometric luminosity, this would not lower the fraction accretion rate. Another concern is that the BLR is in a flat structure, so the velocity depends strongly on the inclination of the system. There is evidence for anisotropy of the BLR velocity in radio-loud AGNs, and the Hβ line width is found to be anticorrelated with the core dominance of the radio source. There is no such radio data for the PKS 0558−504, so it remains possible that we might see a flat BLR from the top in this object, and the mass of the central BH was underestimated. However, the core-dominated radio source usually displays flat spectra as opposed to the steep radio spectrum in these objects (see § 4.1). High-resolution radio observation, however, is necessary to address this.

The other two radio-loud NLS1s (RGB J0044+193 and RX J0134.2−4258) have even lower BH masses and higher accretion rates. Using the same method, we find that the BH masses are $1.6 \times 10^7\ M_\odot$ and $1 \times 10^7\ M_\odot$ for RGB J0044+193 and RX J0134.2−4258, respectively. These two objects show the same characteristics in the spectral energy distribution (SED) as PKS 0558−504: a very big blue bump indicated by its flat optical-UV continuum, huge soft X-ray excess, steep radio spectra, and weak iron K lines (Siebert et al. 1999; Grupe et al. 2000). The mass of RGB J0044+193 can be an order of magnitude larger if the BLR size scales with the luminosity of ionizing continuum instead of the luminosity at 5100 Å and if its extremely steep continuum in the optical spectrum ($\alpha_{\rm opt} \simeq -3.1$; Siebert et al. 1999) extends into the far-UV. However, we notice that the equivalent width of Hβ is normal in this object, suggesting that such a correction is not adequate.

If the above mass estimate is correct, the existence of radio-loud NLS1s suggests that neither a large BH mass nor a low accretion rate is necessary for the formation of a powerful radio jet. So which other factor is relevant: the BH spin or the environment of the galactic nuclei? If a jet is powered by the spin energy of the BH through Blandford & Znajek's (1977) mechanism, both rapid spin of the BH and a strong magnetic field are required for the formation of powerful radio jets. Formation of a rapidly spinning BH in NLS1s can be found in various schemes: a massive hole is formed by the collapse of rotating gas clouds, through the accretion of material by a seeded small hole and the merging of small holes. In particular, the hole spins up very fast in NLS1s, as they are thought to accrete at close to Eddington rate or even at super-Eddington rates. It can easily reach the equilibrium between the spin-up by accretion and the spin-down by the Blandford-Znajek mechanism (Moderski, Sikora, & Lasota 1998), unless the NLS1s phase is extremely short (less than a few times 10^7 years). A strong magnetic field can be either created by the dynamo in the accretion disk or amplified by compressing the convected magnetic field frozen in the accreted material. It remains unexpected that radio-loud NLS1s are so rare.

Alternatively, it was suggested that the observed radio jets are related not only to the center engine but also to the environment of the nuclei, which provides the confinement of the jets. If this is indeed the case, the host galaxies of the radio-loud NLS1s should also be massive elliptical galaxies.

[7] They are formally radio-quiet according to the definition of radio-loudness $R = \log(f_{\rm 5GHz}/f_{\rm opt})$ in AGNs.

We speculate that they deviate from the relationship between BH mass and bulge mass because the BH is still in the rapid-growth phase. We have no data on the bulge masses of these three NLS1s. Nelson & Whittle (1996) suggest that [O III] λ5007 width is a good indicator of stellar velocity dispersion in elliptical galaxies and spiral bulges. The [O III] widths are 670 and 750 km s^{-1} for RX J0134.2−4258 and RGB J0044+193, respectively (Siebert et al. 1999; Grupe et al. 2000), which correspond to stellar velocity dispersions of 285 and 319 km s^{-1}, indicating a massive spheroidal component in both galaxies. This would give BH masses of about 4×10^8–$6 \times 10^8\ M_\odot$ in these two objects if they followed the BH mass and stellar velocity-dispersion relation (see Fig. 1 of Nelson 2000). These masses are 1 order of magnitude larger than the BH masses estimated from the BLR-kinematics method, consistent with our guess. The [O III] is extremely weak in PKS 0558−504 (it has not been given by Corbin 1997) but also seems relatively broad. However, a direct measurement of the stellar velocity dispersion in those objects is needed before any firm conclusions can be drawn.

To summarize, we find that the rapid flare observed in PKS 0558−504 requires an effective radiative efficiency of close to 1. This can be explained either by associating the flare with the relativistic radio jets or with the magnetic heated corona above an accretion disk. Future simultaneous monitoring of this object in radio and X-ray bands would be crucial in discriminating the two possibilities. We showed that a magnetic field of at least a few times 10^4 G in strength is required in the latter case. Future observations with a large photon-collecting areas detector, such as the MAXI program, will allow uninterrupted and detailed monitoring of the spectral evolution of the flare, yielding stringent constraints on the models. We found that the black hole masses in three radio-loud NLS1s are much lower than those in radio-loud quasars, which may suggest that the black holes in narrow-line NLS1s are still in rapid-growth phase.

The authors thank the *ASCA* team for successfully carrying out this observation. T. W. wishes to thank Youjun Lu for many useful comments on an early version of this draft. T. W. acknowledges the financial support of the Chinese NSF through NSF-19925313 and of the Chinese Science and Technology Ministry. This research has made use of the NASA/IPAC Extragalactic Database (NED) which is operated by the Jet Propulsion Laboratory, California Institute of Technology, under contract with NASA.

REFERENCES

Barr, P., & Mushotzky, R. F. 1986, Nature, 320, 421
Beloborodov, A. M. 1999, ApJ, 510, L123
Blandford, R. D., & Begelman, M. C. 1999, MNRAS, 303, L1
Blandford, R. D., & Znajek, R. L. 1977, MNRAS, 179, 433
Boller, T., Brandt, W. N., & Fink H. H. 1996, A&A, 305, 53
Brinkmann, W., Yuan, W., & Siebert, J. 1997, A&A, 319, 413
Catanese, M., & Sambruna, R. M. 2000, ApJ, 534, L39
Corbin, M. R. 1997, ApJS, 113, 245
Corbin, M. R., & Smith, P. S. 2000, ApJ, 532, 136
Fabian, A. C. 1979, Proc. R. Soc. London A, 366, 449
Feigelson, E., et al. 1986, ApJ, 302, 337
Fender, R. P. 2001, MNRAS, 322, 31
Ferrarese, L., & Merritt, D. 2000, ApJ, 539, L9
Forster, K., & Halpern, J. P. 1996, ApJ, 468, 565
Galeev, A. A., Rosner, R., & Vaiana, G. S. 1979, ApJ, 229, 318
Gebhardt, K., et al. 2000, ApJ, 539, L13
Gliozzi, M., Boller, T., Brinkmann, W., & Brandt, W. N. 2000, A&A, 356, L17
Gliozzi, M., Brinkmann, W., O'Brien, P. T., Reeves, J. N., Pounds, K. A., Trifoglio, M., & Gianotti, F. 2001, A&A, 365, L128
Goodrich, R. W. 1989, ApJ, 342, 224
Gotthelf, E. V., Ueda, Y., Fujimoto, R., Kii, T., & Yamaoka, K. 2000, ApJ, 543, 417
Gregory, P. C., Varasour, J. D., Scott, W. K., & Condon, J. J. 1994, ApJS, 90, 173
Grupe, D., Leighly, K. M., Thomas, H. C., & Laurent-Muehleisen, S. A. 2000, A&A, 356, 11
Guilbert, P. W., Fabian, A. C., & Rees, M. J. 1983, MNRAS, 205, 593
Kaspi, S., Smith, P. S., Netzer, H., Maoz, D., Jannuzi, B. T., & Giveon, U. 2000, ApJ, 533, 631
Kataoka, J., Takahashi T., Makino F., Inoue, S., Madejski G. M., Tashiro, M., Urry, C. M., & Kubo, H. 2000, ApJ, 528, 243
Kubo, H., et al. 1998, ApJ, 504, 693
Laor, A. 2000, ApJ, 543, L111
Leighly, K. 1999a, ApJS, 125, 297
———. 1999b, ApJS, 125, 317
Magorrian, J., et al. 1998, AJ, 115, 2285
McHardy, I. M. 1989, in 23rd ESLAB Symp. Proc., ed. J. Hunt & B. Battrick (Paris: ESA), 499
McLure, R. J., Kukula, M. J., Dunlop, J. S., Baum, S. A., O'Dea, C. P., & Hughes, D. H. 1999, MNRAS, 308, 377
Mineshige, S., Kawagichi, T., Takeuchi, M., & Hayashida, K. 2000, PASJ, 52, 499
Moderski, R., Sikora, M., & Lasota, J. P. 1998, MNRAS, 301, 142
Nandra, K. et al. 1997, ApJ, 476, 70
Nelson, C. H. 2000, ApJ, 544, L91
Nelson, C. H., & Whittle, M. 1996, ApJ, 465, 96
O'Brien, P. T., et al. 2001, A&A, 365, L122
Osterbrock, D. E., & Pogge, R. W. 1985, ApJ, 297, 166
Otani, C., Kii, T., & Miya, K. 1996, in Röntgenstrahlung from the Universe, ed. H. U. Zimmermann, J. E. Trümper, & H. Yorke (Garching: MPE), 491
Rees, M. J. 1984, ARA&A, 22, 471
Rees, M. J., Begelman, M. C., Blandford, R. D., & Phiney, E. S. 1982, Nature, 295, 17
Remillard, R. A., Grossan, B., Bradt, H. V., Ohashi, T., Hayashida, K., Makino, F., & Tanaka, Y. 1992, Nature, 350, 589
Siebert, J., Leighly, K. M., Laurent-Muehleisen, S. A., Brinkmann, W., Boller T., & Matsuoka, M. 1999, A&A, 348, 678
Tanaka, Y., Inou, H., & Holt, S. S. 1994, PASJ, 46, L37
Worrall, D. M., & Wilkes, B. J. 1990, ApJ, 360, 396
Wright, A. E., Griffith, M. R., Burker, B. F., & Ekers 1994, ApJS, 91, 111
Wright, A., & Otrupcek, R. 1990, Parkes Catalogue, Australia Telescope National Facility